

Geomagnetic Positioning-Aided Wi-Fi FTM Localization Algorithm for NLOS Environments

Meng Sun, Yunjia Wang, Lu Huang, Haonan Jia, Jingxue Bi,
Wout Joseph and David Plets

Abstract—WiFi-based indoor localization using the fine time measurement (FTM) protocol has become a popular technique. However, in harsh Non-Line-of-Sight (NLoS) environments, WiFi FTM positioning (WFP) suffers from poor performance. In this letter, a novel WiFi FTM localization method with the assistance of geomagnetic positioning (GP) is proposed. To ensure the accuracy of GP, an enhanced mind evolutionary algorithm (EMEA) is designed. A fine-grained WiFi position estimation method using the overlapping searching area (OSA) and the coincident points selection strategy is proposed. Experimental results show that the EMEA-based GP improves the localization performance of WFP in NLOS environments, the mean localization error (ME) and root-mean-square error (RMSE) of the GP-aided WFP are 1.82 m and 2.08 m, respectively. Compared with the classic WFP using the weighted least square (WLS) method, the ME and RMSE are reduced by 51.7% and 52.4%, respectively.

Index Terms—Indoor localization, WiFi FTM, magnetic positioning, NLOS, mind evolutionary algorithm.

I. INTRODUCTION

LOCALIZATION using MIMO [1], [2] and WiFi [3] to determine the positions of the objects indoors is very popular. Recently, positioning using the WiFi FTM has attracted extensive attention. Meter-level WiFi ranging accuracy in Line-of-Sight (LoS) environments is reported in [4]. However, complex indoor topologies lead to serious NLoS errors on WiFi ranging. NLoS/LoS identification [5] can help improve accuracy, but it remains difficult to execute the identification methods during online positioning. To improve localization precision, different algorithms have been proposed, such as WiFi FTM with map information fusion [6], WiFi path loss model range and FTM range fusion [7], WiFi FTM and built-in sensors integration [8], [9], and WiFi FTM localization using

a temporal-spatial constraint strategy [10]. Apart from using sensor fusion or map information, it is necessary to develop efficient methods to limit the NLoS influence on localization using the available signals in indoor environments.

For addressing this problem, we propose a WFP method with the assistance of geomagnetic positioning (GP). Performing GP in all indoor environments is feasible and efficient based on the pervasiveness of the magnetic field (MF) [11], [12]. The advantage of GP is that it does not suffer from NLoS or multipath problems. If the Wi-Fi signals are denied or the WiFi ranging is not accurate in NLoS environments, GP could be a good supplementary solution for accurate position estimation. Based on this assumption, we design a GP-aided WFP method and conduct extensive experiments in an NLoS environment to evaluate it. Our contributions are summarized as follows:

- 1) We propose a novel GP approach based on an EMEA. This EMEA-based GP can quickly search for the optimal magnetic position and provide a good searching area for the NLoS limitation in WFP.
- 2) We design the overlapping searching area and coincident points selection strategies to mitigate the NLoS effects on the localization accuracy of WFP by merging the EMEA-based GP and WiFi measurements.
- 3) We conduct extensive experiments to test the proposed methods and confirm that using the EMEA-based GP to improve the accuracy of WFP in NLoS environments is feasible and efficient.

II. RELATED WORKS

In LoS/low-multipath environments, meter-level WiFi ranging is confirmed in [4], but it also reports that the WiFi ranging and localization precision collapse in NLoS scenarios. To address this problem, an LoS/NLoS recognition method is studied in [5], which can work well in a mixed LoS/NLoS scenario, but cannot be successfully executed in a complete NLoS environment. Alternatively, map information and WFP fusion is studied in [6] and achieved an accuracy of 3 m in 90% of the cases. In [7], an RSS-based range and FTM range fusion is proposed and the reported accuracy improvement is 30.4%. In [8] and [9], researchers built WFP and pedestrian dead reckoning (PDR) fusion models and the reported accuracy is meter-level. However, these works are done in a low-NLoS environment and PDR plays a leading role in the fusion system. An efficient WFP in a complicated environment still needs to be studied.

Complex NLoS indoor topologies lead to the discernibility of MF and provide special features for GP [11]. Performing GP requires constructing a magnetic map as in [12] or storing the magnetic patterns as the reference targets in [13].

This work was supported by the National Key Research and Development Program of China under Grant 2016YFB0502102, in part by the China Scholarship Council under Grant CSC 202006420023, in part by the National Natural Science Foundation of China (No.42001397), and in part by the Postgraduate Research & Practice Innovation Program of Jiangsu Province under Grant KYCX21_2293. The associate editor coordinating the review of this letter and approving it for publication was A. Guerra. (Corresponding author: Yunjia Wang.)

Meng Sun and Yunjia Wang are with the Key Laboratory of Land Environment and Disaster Monitoring, MNR, School of Environment and Spatial Informatics, China University of Mining and Technology, Xuzhou 221116, China (e-mail: msun@cumt.edu.cn; wyjc411@163.com).

Lu Huang and Haonan Jia are with the State Key Laboratory of Satellite Navigation System and Equipment Technology, Shijiazhuang 050081, China (e-mail: hlccct54@163.com; jiahaonan1022@163.com).

Jingxue Bi is with the College of Surveying and Geo-informatics, Shandong Jianzhu University, Jinan 250101, China (e-mail: bijingxue19@sdjzu.edu.cn).

Wout Joseph and David Plets are with the WAVES Group, Department of Information Technology, Ghent University, 9052 Ghent, Belgium (e-mail: David.Plets@ugent.be; Wout.Joseph@ugent.be).

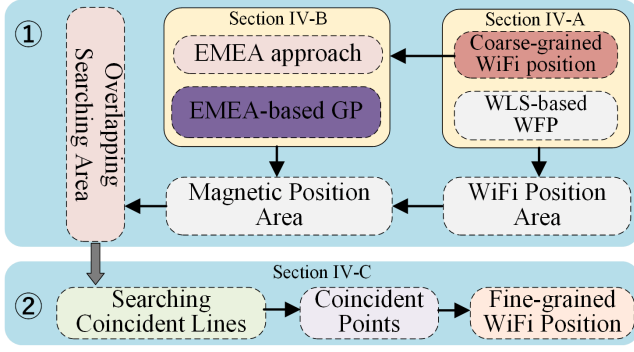


Fig. 1. The structure of EMEA-based GP-aided Wi-Fi FTM Localization.

Magnetic patterns are used for localization based on a convolutional neural network (CNN) in [13] and can localize a user within 1.01 m in 75% of the cases. Other positioning algorithms including sensitivity-based adaptive particle filter [14], stochastic magnetic matching [15], etc., have been studied and can obtain good performance. Performing GP without considering the NLOS problems makes it very suitable as a supplementary solution for the accuracy improvement of WFP in NLoS environments.

III. ALGORITHM ARCHITECTURE

Fig.1 shows that the proposed EMEA-based GP-aided WiFi FTM localization algorithm contains two phases: the overlapping searching area (OSA) selection and the fine-grained WiFi position estimation. When determining OSA, a coarse-grained WiFi position is first calculated based on the weighted least square (WLS) algorithm. A square area around this coarse-grained position is defined. Then, a partial magnetic database is selected and the GP using an EMEA is executed. Similarly, a square magnetic position area can also be selected. The OSA is the overlapping area of these two areas. Then, based on this OSA, we design the coincident lines and points searching strategy to find the candidates positions for the fine-grained WiFi position estimation. More details about the used methods at different phases are described in Section IV.

IV. METHODS

A. WiFi FTM Ranging and Positioning

As Fig.2 shows, the phone starts with sending an FTM request to an access point (AP) and one ACK message is sent back if the AP responds to this FTM request. After this initial response, the AP will send the FTM package to the phone and record the ToD (time-of-departure) $t_1(1)$. If the phone receives the FTM package, it records the ToA (time-of-arrival) $t_2(1)$ and returns the ACK message to the AP. Similarly, the ToD $t_3(1)$ and ToA $t_4(1)$ of the ACK package are recorded by the phone and the AP, respectively. Then, one FTM exchange is completed. If there are n exchanges within one second, the mean round-trip-time (RTT) of the WiFi signal flight is calculated as:

$$RTT = \frac{1}{n} \sum_{k=1}^n ([t_4(k) - t_1(k)] - [t_3(k) - t_2(k)]) \quad (1)$$

The theoretical WiFi ranging model is expressed as follows:

$$r = \frac{C}{2n} \times \sum_{k=1}^n ([t_4(k) - t_1(k)] - [t_3(k) - t_2(k)]) \quad (2)$$

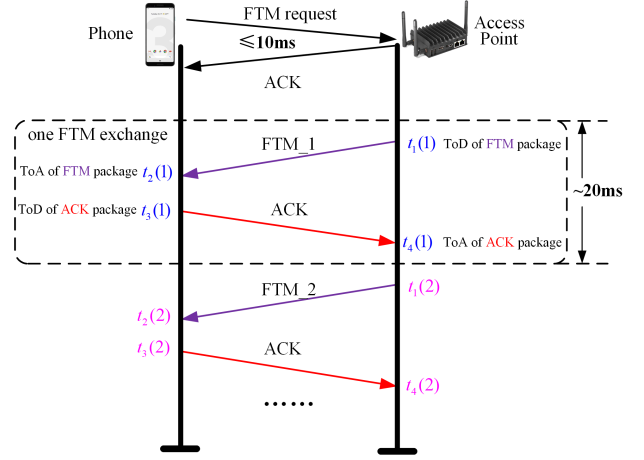


Fig. 2. WiFi FTM producer.

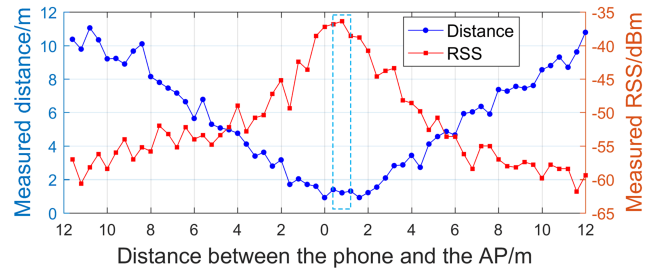


Fig. 3. The measured distance and RSS when tester moves from one end of the AP to the other end.

where r is the distance between the phone and an AP, $C = 3 \times 10^8 m/s$, n is the number of successful FTM exchanges within one second.

We first perform coarse-grained WFP using FTM ranging data based on the WLS algorithm in [16]. In this letter, we further introduced the access point detection (APD) producer into the WFP by using the WiFi received signal strength (RSS) and ranging data. The APD strategy is used for position correction. If an AP is detected, the WiFi and magnetic positions will be corrected by assigning the recorded coordinates of the detected AP. Fig.3 shows that the WiFi ranging data will increase from the minimal to the maximal values as the tester gradually moves away from the AP. An AP is classified as detected if all the conditions of (3) is met:

$$\begin{cases} r_i < r_t \& RSS_i > RSS_t \\ r_{i-1} > r_i \& r_{i+1} > r_i \\ RSS_{i-1} < RSS_i \& RSS_{i+1} < RSS_i \end{cases} \quad (3)$$

where r_t and RSS_t are thresholds, which are set as 2 m and -45 dBm, respectively; $r_i, r_{i-1}, r_{i+1}, RSS_i, RSS_{i-1}, RSS_{i+1}$ are the ranging data and RSS between the phone and an AP at the time $i, i-1, i+1$, respectively.

B. EMEA-Based Geomagnetic Positioning

1) *Enhanced Mind Evolutionary Algorithm*: The mind evolutionary algorithm (MEA) is a popular searching algorithm [17]. In this letter, we design an enhanced MEA (EMEA) with a subgroups number setting (SNS) strategy that can adaptively assign the numbers of subgroups. As Fig.4 shows, EMEA needs a population to perform evolution. The individuals of the population get different scores based on their fitness

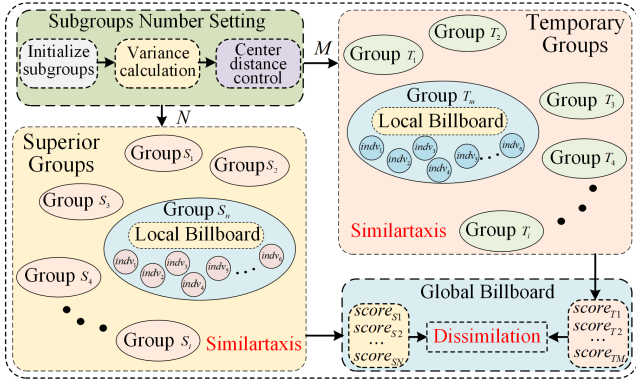


Fig. 4. Enhanced mind evolutionary algorithm.

to the searching space. After performing SNS, the numbers of superior and temporary subgroups are obtained, then EMEA executes the similartaxis and dissimilation operators to find the optimal result. The evolution process is as follows:

Step 1 (Initialize Subgroups): After the population is generated, individuals' scores are calculated. The ones with the highest scores are selected as the centers. A group is generated around the centers with a random distribution.

Step 2 (Variance Calculation): This step is to make the distribution of individuals within one group more concentrated. If a subgroup is expressed as $\{z_i, i = 1, 2, 3, \dots, n\}$, the variance is calculated as:

$$var = \frac{1}{n} \sum_{i=1}^n (z_i - \bar{z})^2 \quad (4)$$

where \bar{z} is the mean value of the subgroup. Then, a subgroup is divided if the variance is higher than the threshold.

Step 3 (Center Distance Control): This step is to make all groups uniformly distributed. Two subgroups are combined if the center distance is smaller than the threshold, and a new group is regenerated in the searching space.

Step 2 and Step 3 are executed until no groups are divided or combined. The remaining groups will be assigned as the superior and temporary groups. If the numbers of superior and temporary groups are N and M , and the number of total subgroups is T , N and M satisfy the condition in (5) and are updated by using (6):

$$T = N + M \quad (5)$$

$$\begin{cases} N = N + 1, & s_{imax} < \delta \\ M = M + 1, & s_{imax} > \delta \end{cases} \quad (6)$$

where s_{imax} is the maximal score of the i -th subgroups, δ is a threshold, T is set to 10 in this work.

Step 4 (Similartaxis and Local Competition): This step is to make the subgroup mature. The individuals within one group compete by comparing scores. If the difference of the maximal and minimal scores satisfies the mature condition, this group is mature and its maximal score is posted on the global billboard.

Step 5 (Dissimilation and Global Competition): If all the subgroups are mature, dissimilation executes global competition by comparing the posted scores on the global billboard. The temporary groups with higher scores replace the superior groups with lower scores. New temporary groups are regenerated in the searching space.

All the above steps are executed cyclically until no superior groups are replaced or the number of iterations reaches the maximal iteration number. The individual with the highest score in the superior groups is selected as the final result.

2) *Geomagnetic Positioning Using EMEA:* Many temporary magnetic positions (MP) can be obtained because of the high sampling rate of the magnetometer. These positions constitute a population for performing EMEA. If the sampling rate is n Hz and the MP population at the time k is $\mathbf{P}(k)$:

$$\mathbf{P}(k) = \{m_k(x_1, y_1), \dots, m_k(x_i, y_i), \dots, m_k(x_n, y_n)\} \quad (7)$$

where $m_k(x_i, y_i)$ is the i -th individual of $\mathbf{P}(k)$ with the coordinate values $(x_i, y_i), i = 1, 2, \dots, n$. The evolution process in the EMEA occurs via comparison of the individuals' scores, which are related to the previous estimated true MP (X_{k-1}, Y_{k-1}) and calculated as:

$$s\{k, i\} = \frac{1}{\sqrt{(X_{k-1} - x_i)^2 + (Y_{k-1} - y_i)^2}} \quad (8)$$

In (8), $s\{k, i\}$ will be set to 0 if (x_i, y_i) is the same as (X_{k-1}, Y_{k-1}) . After the subgroups initialization, the variance calculation can be defined as:

$$var = \frac{1}{n} \sum_{i=1}^n [(x_i - \bar{x})^2 + (y_i - \bar{y})^2] \quad (9)$$

where \bar{x} and \bar{y} are the mean coordinate values of all the individuals' positions within one subgroup. If the variance is larger than 0.5 in this work, this subgroup is divided into two groups. The next step of SNS is to calculate the center distance of two subgroups. If the center distance is smaller than 1 m, two subgroups are combined. After the SNS strategy is performed, superior and temporary subgroups are obtained. Then, the similartaxis and dissimilation operations are executed. A group is mature if (10) is met:

$$|s\{k, i\}_{max} - s\{k, i\}_{min}| < \epsilon \quad (10)$$

where ϵ is set to 0.5 in this work. When EMEA meets the convergence condition, the best individual of the superior group is selected as the estimated MP.

C. Fine-Grained WiFi Position Estimation

Before performing the localization algorithm, a division of the positioning area into grid points needs to be made. These points are used for the OSA selection. After performing the WLS-based WFP and EMEA-based GP, the OSA can be obtained as shown in Fig.5(a). The grid points in OSA are the candidates for the fine-grained position estimation. Fig.5(b) shows the coincident lines and points searching process. First, the Euclidean distance l_i between the candidate point and AP is calculated. In theory, the angle between two lines is 0° if they are coincident. If assigning another side length ζ , a triangle can be obtained together with l_i and the measured distance r_i . The angle θ between l_i and r_i is calculated as:

$$\theta_i = \arccos\left(\frac{l_i^2 + r_i^2 - \zeta^2}{2l_i r_i}\right) \quad (11)$$

where ζ is set to 1. If θ is infinitely close to 0° , l_i and r_i are coincident and the grid point which is used for calculating l_i

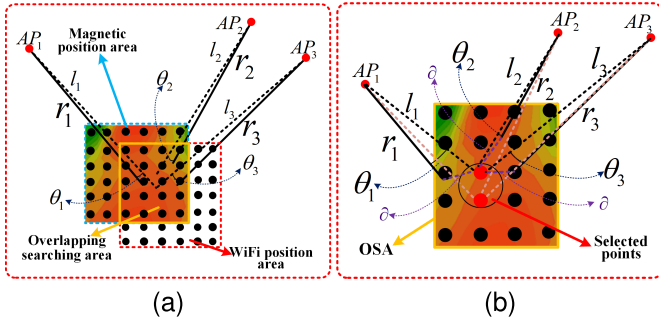


Fig. 5. The details of OSA and coincident points selection. (a) OSA selection, (b) Coincident points selection.

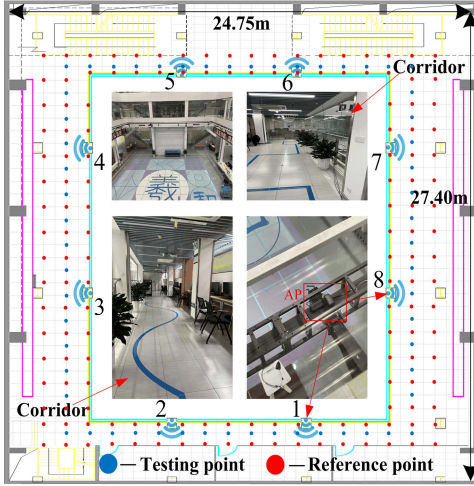


Fig. 6. Experimental area.

is selected as a coincident point (CP). Using one AP to search in OSA can obtain a CP set. Several CP sets will be selected if all APs finish searching. Finally, the same points among these CP sets are selected and the mean coordinates values of these same points are calculated as the final estimated position.

V. EXPERIMENTS

A. Experimental Setup

As Fig.6 shows, the experimental area is more than 650 square meters. 8 WiFi APs with the hardware part of Intel Dual Band Wireless-AC8260 are installed. They are outside of the corridors and cannot be directly observed from the corridors or rooms, which means that the WiFi ranging is always executed in a NLoS condition. The magnetic features are collected at 166 reference points with an interval of 1.2 m. Then, 1756 grid points with an interval of 0.3 m are obtained using a linear interpolation method and the corresponding magnetic features are also interpolated. Testing data are recollected three times at 64 testing points using a Pixel 3 phone with a sampling rate of 50 Hz and 5 Hz for the magnetometer and WiFi ranging, respectively. 7 APs responded to the FTM request except for the No.5 AP during the test. All the data are analyzed on a laptop with 8 GB RAM and a 2.6GHz CPU.

B. Geomagnetic Positioning Comparison

We first investigate the performance of the improved GP by comparing it to the GP methods using the MEA and k-nearest neighbors (KNN). As shown in Tab. I, compared to the MEA

TABLE I
ERRORS COMPARISON OF GEOMAGNETIC POSITIONING ALGORITHMS

Algorithm	Min/m	Max/m	Mean/m	RMSE/m	75%Error/m
EMEA	0.34	9.45	2.21	2.72	2.63
MEA	0.41	11.47	2.59	3.38	3.03
KNN	0.39	13.68	3.06	3.90	4.07

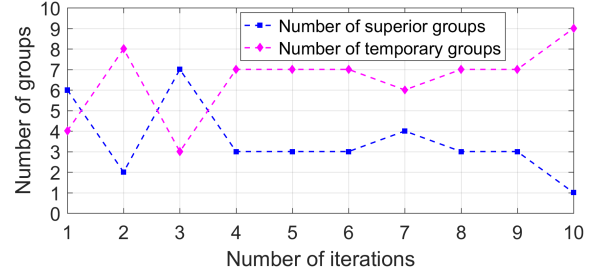


Fig. 7. Subgroup numbers dynamic adaptation.

TABLE II
ERRORS COMPARISON OF WiFi POSITIONING METHODS

Methods	Min/m	Max/m	Mean/m	RMSE/m	75%Error/m
EMEA-WLS	0.10	5.43	1.82	2.08	2.51
MEA-WLS	0.13	6.71	2.19	2.57	2.84
KNN-WLS	0.15	9.91	2.62	3.17	3.23
RSS-FTM	0.32	11.35	3.25	3.74	4.17
WLS	0.37	11.20	3.77	4.37	5.09

and KNN, the EMEA obtains a localization accuracy of 2.21m, which is improved by about 0.38 m and 0.85 m, and the root-mean-square error (RMSE) is also reduced by 0.66 m and 1.18 m, respectively. Fig.7 shows that the subgroup's numbers are adaptively assigned when every time EMEA runs. We can conclude that the SNS strategy improves the classic MEA's capability, and the EMEA-based GP can obtain good results.

C. WiFi FTM Positioning Methods Comparison

We now compare the EMEA-based GP-aided WFP with the WLS-based WFP in [16], the RSS-based range/FTM fusion in [7], the WLS-based WFPs with the MEA-based GP and KNN-based GP. We denote these approaches as EMEA-WLS, WLS, RSS-FTM, MEA-WLS, and KNN-WLS, respectively.

Tab. II shows that the mean error (ME) and RMSE of EMEA-WLS are 1.82 m and 2.08 m, respectively, which are reduced by 51.7% and 52.4% compared with the WLS. This result clearly shows that the WiFi location accuracy is improved with the assistance of GP. The same conclusion can be drawn by comparing the MEA-WLS and KNN-WLS with WLS. Under the same confidence level of 75%, the GP-aided WFP methods also have better performance than the single WFP. Using the RSS-FTM approach in [7] can also improve the precision of WLS, albeit with an improvement of only 13.8% for the considered data set. However, using magnetic signals can obtain a higher improvement of 51.7%. Moreover, compared with the results of EMEA-based GP in Tab.I, the ME and RMSE of EMEA-WLS are also reduced by 17.6% and 23.5%, respectively.

D. Impact of Number of APs on Accuracy

We also investigate the impact of the number of APs on the positioning accuracy of the methods in Section C.

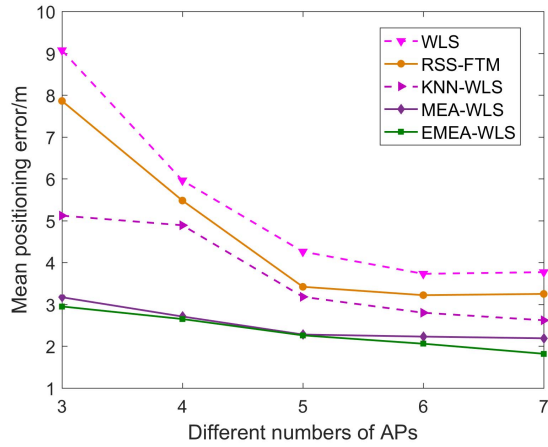


Fig. 8. Mean positioning errors of different methods using different numbers of APs.

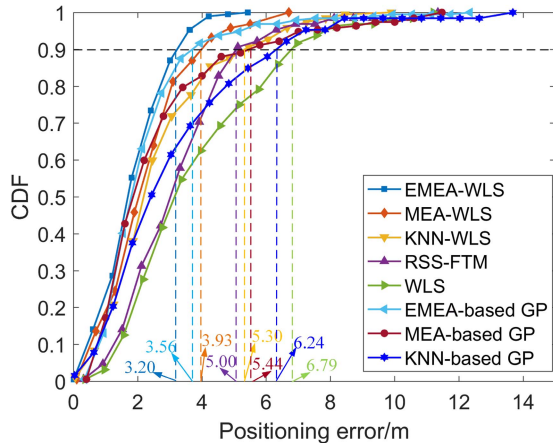


Fig. 9. CDFs comparison of different methods.

Different AP combinations are selected as follows: 3 APs (No.1,3,7), 4 APs (No.1,3,4,7), 5 APs (No.1,3,4,6,7), and 6 APs (No.1,3,4,6,7,8). Fig.8 shows that the mean positioning error of these methods gradually decreases as the number of APs increases. When 3 APs are used, WLS only obtains a localization accuracy of about 9 m. However, performing RSS-FTM, KNN-WLS and MEA-WLS can help to improve precision, with EMEA-WLS having the largest accuracy improvement, which is about 6 m. The same conclusion can be drawn when comparing the accuracy improvement of these approaches using more APs. We conclude that the EMEA-WLS can keep good performance in NLoS environments when fewer APs are used.

E. Comparison of Positioning Methods and Discussion

For a confidence level of 90%, Fig.9 shows that only performing WLS-based WFP or KNN-based GP cannot obtain good results with localization errors larger than 6.20 m. The positioning accuracy of GP gradually increases when using the KNN, MEA, and EMEA. This also shows the effectiveness of the EMEA. With the assistance of the three GPs, the WFP's precision also gradually increases, and the proposed EMEA-WLS gets the best result, which is 3.20 m in 90% of the cases. From the perspective of accuracy improvement, EMEA-WLS shows an improvement of 51.7% as discussed in

Section C. This result is better than that of using NLoS identification in [5] with an improvement of 36.4% and inputting RSS/FTM data in [7] with an improvement of 13.8%. With a denser AP deployment, the RSS-based fingerprinting in [3] obtained a higher precision. Its reported accuracy improvement equals 16.7%. Experiments prove that using GP to improve the WFP's accuracy is feasible and efficient.

VI. CONCLUSION

In this letter, we propose to use GP to improve the accuracy of WFP in NLoS environments. Experiments verify the feasibility of our method and testing results show that the GP-aided WFP can obtain a location accuracy of 1.82 m, which is improved by nearly 52% compared with the traditional WLS method. In the future, we will further study using WiFi RSS and smartphone build-in sensors to improve precision, and using barometers to realize 3D localization.

REFERENCES

- [1] A. Guerra, F. Guidi, and D. Dardari, "Single-anchor localization and orientation performance limits using massive arrays: MIMO vs. beam-forming," *IEEE Trans. Wireless Commun.*, vol. 17, no. 8, pp. 5241–5255, Aug. 2018.
- [2] Y. Wang, Y. Wu, and Y. Shen, "Joint spatiotemporal multipath mitigation in large-scale array localization," *IEEE Trans. Signal Process.*, vol. 67, no. 3, pp. 783–797, Feb. 2019.
- [3] C. Feng, W. S. A. Au, S. Valaee, and Z. Tan, "Received-signal-strength-based indoor positioning using compressive sensing," *IEEE Trans. Mobile Comput.*, vol. 11, no. 2, pp. 1983–1993, Dec. 2012.
- [4] K. Jiokeng, G. Jakllari, A. Tchana, and A.-L. Beylot, "When FTM discovered MUSIC: Accurate WiFi-based ranging in the presence of multipath," in *Proc. IEEE Conf. Comput. Commun. (INFOCOM)*, Jul. 2020, pp. 1857–1866.
- [5] M. Si, Y. Wang, S. Xu, M. Sun, and H. Cao, "A Wi-Fi FTM-based indoor positioning method with LOS/NLoS identification," *Appl. Sci.*, vol. 10, no. 3, p. 956, Feb. 2020.
- [6] L. Banin, U. Schatzberg, and Y. Amizur, "Wifi FTM and map information fusion for accurate positioning," in *Proc. IPIN*, 2016, pp. 1–4.
- [7] G. Guo, R. Chen, F. Ye, X. Peng, Z. Liu, and Y. Pan, "Indoor smartphone localization: A hybrid WiFi RTT-RSS ranging approach," *IEEE Access*, vol. 7, pp. 176767–176781, 2019.
- [8] S. Xu, R. Chen, Y. Yu, G. Guo, and L. Huang, "Locating smartphones indoors using built-in sensors and Wi-Fi ranging with an enhanced particle filter," *IEEE Access*, vol. 7, pp. 95140–95153, 2019.
- [9] Y. Yu *et al.*, "Precise 3-D indoor localization based on Wi-Fi FTM and built-in sensors," *IEEE Internet Things J.*, vol. 7, no. 12, pp. 11753–11765, Dec. 2020.
- [10] W. Shao, H. Luo, F. Zhao, H. Tian, S. Yan, and A. Crivello, "Accurate indoor positioning using temporal-spatial constraints based on Wi-Fi fine time measurements," *IEEE Internet Things J.*, vol. 7, no. 11, pp. 11006–11019, Nov. 2020.
- [11] S. He and K. G. Shin, "Geomagnetism for smartphone-based indoor localization: Challenges, advances, and comparisons," *ACM Comput. Surv.*, vol. 50, no. 6, pp. 1–37, 2017.
- [12] G.-X. Liu, L.-F. Shi, S. Chen, and Z.-G. Wu, "Focusing matching localization method based on indoor magnetic map," *IEEE Sensors J.*, vol. 20, no. 17, pp. 10012–10020, Sep. 2020.
- [13] I. Ashraf, M. Kang, S. Hur, and Y. Park, "MINLOC: Magnetic field patterns-based indoor localization using convolutional neural networks," *IEEE Access*, vol. 8, pp. 66213–66227, 2020.
- [14] M. Zheng, Y. Zhao, Y. He, and C.-Z. Xu, "Sensitivity-based adaptive particle filter for geomagnetic indoor localization," in *Proc. IEEE/CIC Int. Conf. Commun. China (ICCC)*, Oct. 2017, pp. 1–6.
- [15] L. Hou *et al.*, "Orientation-aided stochastic magnetic matching for indoor localization," *IEEE Sensors J.*, vol. 20, no. 2, pp. 1003–1010, Jan. 2020.
- [16] M. Sun, Y. Wang, S. Xu, H. Qi, and X. Hu, "Indoor positioning tightly coupled Wi-Fi FTM ranging and PDR based on the extended Kalman filter for smartphones," *IEEE Access*, vol. 8, pp. 49671–49684, 2020.
- [17] C. Sun, Y. Sun, and W. Wang, "A survey of MEC: 1998–2001," in *Proc. IEEE Int. Conf. Syst., Man Cybern.*, vol. 6, Oct. 2002, pp. 445–453.